

Landslides (2008) 5:445–455
 DOI 10.1007/s10346-008-0133-4
 Received: 23 November 2007
 Accepted: 24 March 2008
 Published online: 17 July 2008
 © Springer-Verlag 2008

Panya S. Lipovsky · Stephen G. Evans · John J. Clague · Chris Hopkinson · Réjean Couture · Peter Bobrowsky · Göran Ekström · Michael N. Demuth · Keith B. Delaney · Nicholas J. Roberts · Garry Clarke · Andrew Schaeffer

The July 2007 rock and ice avalanches at Mount Steele, St. Elias Mountains, Yukon, Canada

Abstract A large rock and ice avalanche occurred on the north face of Mount Steele, southwest Yukon Territory, Canada, on July 24, 2007. In the days and weeks preceding the landslide, several smaller avalanches initiated from the same slope. The ice and rock debris traveled a maximum horizontal distance 5.76 km with a maximum vertical descent of 2,160 m, leaving a deposit 3.66 km² in area on Steele Glacier. The seismic magnitude estimated from long-period surface waves (M_s) is 5.2. Modeling of the waveforms suggests an estimated duration of approximately 100 s and an average velocity of between 35 and 65 m/s. This landslide is one of 18 large rock avalanches known to have occurred since 1899 on slopes adjacent to glaciers in western Canada. We describe the setting, reconstruct the event chronology and present a preliminary characterization of the Mount Steele ice and rock avalanches based on field reconnaissance, analysis of seismic records and an airborne LiDAR survey. We also present the results of a successful dynamic simulation for the July 24 event.

Keywords Rock avalanche · Ice avalanche · Mount Steele · St. Elias Mountains · Yukon Territory

Introduction

In July 2007, multiple avalanches involving rock and ice occurred on the steep glaciated northern slope of Mount Steele, Yukon Territory, Canada, depositing a large volume of rock debris and ice on the surface of Steele Glacier (Fig. 1). Seismograph records and eyewitness observations indicate at least three rock and ice avalanches occurred between July 22 and July 24, 2007. Two or more smaller debris flows occurred on the same slope prior to July 22. The largest of the avalanches, referred to hereafter as the “main event”, took place at 1825 hours local time on July 24 (July 25, 00:57 UTC). It is one of 18 large rock avalanches onto glaciers that have been documented in the Canadian Cordillera since 1899 (Evans and Clague 1999) and one of a much larger number that have occurred on glaciers in the mountains of northwest North America since 1964 (Post 1967; Jibson et al. 2006; Molnia et al. 2006).

The objectives of this report are threefold: (1) to describe the geographic and geologic setting of the July 2007 rock and ice avalanches at Mount Steele; (2) to provide an initial chronology and characterization of the events based on reconnaissance field observations, interpretation of an aerial LiDAR survey and analysis of seismological data; and (3) to discuss the regional and global significance of the avalanches.

Geographic and geologic setting

Standing 5,067 m above sea level (asl), Mount Steele (61°05'35.4" N, 140°18'38.4" W) is the fifth highest mountain in Canada and the tenth highest peak in North America. It is located in Kluane National Park in an uninhabited region of southwest Yukon

Territory (Fig. 2). The mountain lies within the Icefield Ranges of the St. Elias Mountains, an area of high, rugged, snow- and ice-covered mountains surrounded by valley glaciers.

The source of the 2007 ice and rock avalanches is the north face of Mount Steele, which rises over 2,100 m above upper Steele Glacier (Figs. 1, 2 and 3). This face is almost entirely covered by glacier ice and firn estimated to be 30 m thick on average.

Steele Glacier extends approximately 35 km from its source near Mount Steele to its terminus at 1,160 m asl. It has a history of surges, the most recent of which occurred between 1965 and 1968 (Stanley 1969, 1972). Steele Creek flows from the glacier toe to its confluence with the Donjek River 12 km to the east (Fig. 2).

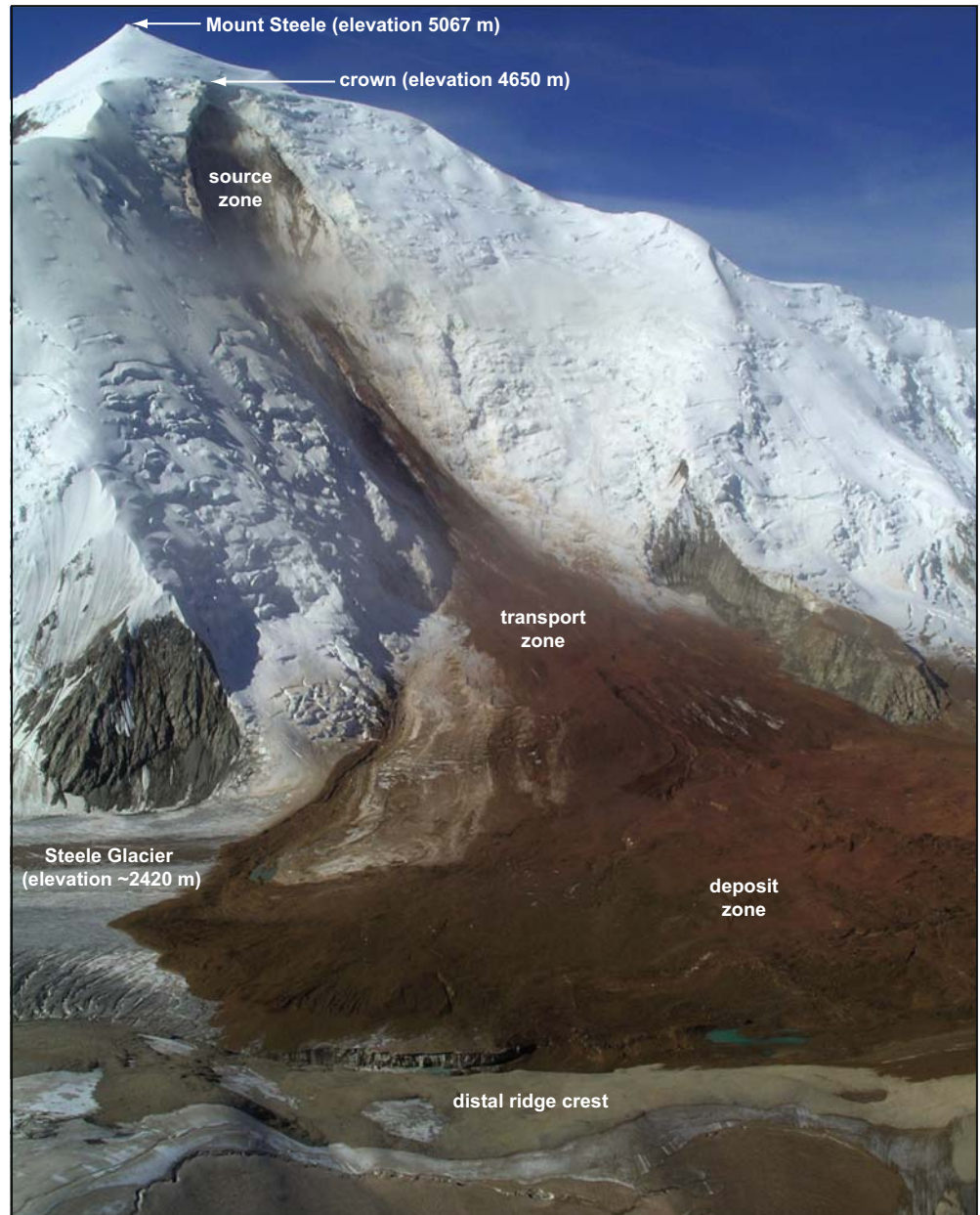
The Alaska Highway crosses the Donjek River about 52 km downstream from the glacier terminus (Fig. 2). It is Yukon's main highway and parallels the proposed route of a pipeline that will carry natural gas southward from the North Slope of Alaska to markets in the conterminous USA. Burwash Landing (population ~100) is the nearest settlement to Mount Steele, 76 km northeast of the peak.

Burwash Landing (807 m asl) has a semi-arid continental climate, with mean annual precipitation of 280 mm and mean annual temperature of -3.8°C (Environment Canada normals for 1971–2000). Mean annual temperature decreases with elevation in the eastern and northern parts of the St. Elias Mountains to about -9°C at 2,500 m and -22°C at 5,000 m (Smith et al. 2004). Mean annual temperature at a weather station located at 2,670 m, 52 km southeast of Mount Steele, ranged from -8.8°C to -9.5°C between 2003 and 2005 (C. Zdanowicz, unpublished data).

The St. Elias Mountains are rapidly rising due to plate interactions off the south coast of Alaska (Bruhn et al. 2004). The Denali and Duke River faults extend northwest through the region east and north of Mount Steele (Fig. 2). The Denali fault system within Canada has been inactive during the late Holocene (Clague 1979), but at least 350 km of right-lateral offset occurred during the Cenozoic (Lowey 1998). Active seismicity and release of strain along the main Denali Fault in Alaska are transferred to the Totshunda and Duke River fault systems in Canada, resulting in moderate to large earthquakes in the St. Elias Mountains (Horner 1983; Everard and Savigny 1994; Haeussler et al. 2004). Rapid uplift and erosion by glaciers, streams and landslides are responsible for the extreme relief in the St. Elias Mountains (Pavlis et al. 2004; Spotila et al. 2004).

The geology of the Mount Steele area has not been mapped in detail, but regional-scale mapping indicates that the rocks on the north face of Mount Steele consist of granodiorite, diorite and gabbro of the Late Miocene Wrangell Suite (Dodds and Campbell 1992). The Wrangell Suite intrudes late Proterozoic to Triassic volcanic and sedimentary rocks of the Alexander Terrane (Gordev and Makepeace 2003; Wheeler et al. 1991; Dodds and Campbell 1992).

Fig. 1 Oblique aerial photo showing the north face of Mount Steele and the July 24th rock and ice avalanche path (photo by P. von Gaza, August 2, 2007). View is to the southwest



Event chronology

The 2007 rock and ice avalanches occurred within a steep gully system on the north face of Mount Steele (Figs. 1, 3 and 4). Previous mass movements at this site suggest the existence of conditions favourable for slope failure. Photographs taken during scientific expeditions in the late 1930s, for example, show fresh debris in the gully system (Wood 1972; F. Wood, unpublished data, 1939). The bowl-shaped morphology of the north face of Mount Steele suggests that large landslides have occurred there repeatedly in earlier times.

The events in July 2007 have been remarkably well-documented, given the remoteness of the locality and difficulty of access. Glaciologists flying to Trapridge Glacier on July 14, 2007 took photos of Mount Steele's north face showing fresh debris in the gully system. The glaciologists also observed a large crevasse that had developed in the ice above the gully system (Fig. 5a). Photos of the

lower part of the north face taken by a park warden on July 21 show deposits of at least two fresh debris flows. One of the debris flows traveled partway down the tributary glacier, while the other traveled further and reached the southwest margin of Steele Glacier (Fig. 6a).

On July 22, at approximately 1325 hours local time (Pacific Daylight Time), the glaciologists at Trapridge Glacier witnessed a large ice avalanche on the north face of Mount Steele. A slab of ice, ~3 million cubic metres in volume, broke away along the crevasse noted a week earlier (Fig. 5a, b). The slab rapidly fragmented and developed into an avalanche that entrained additional snow and ice as it swept down the system of gullies onto Steele Glacier. The leading edge of the avalanche powder cloud traveled across Steele Glacier, up a 275-m-high ridge and down onto Hodgson Glacier, a total horizontal distance of at least 8 km (Figs. 3 and 4). The avalanche debris covered an area of about 2 km² on Steele Glacier (Fig. 6b), and the distal edge of

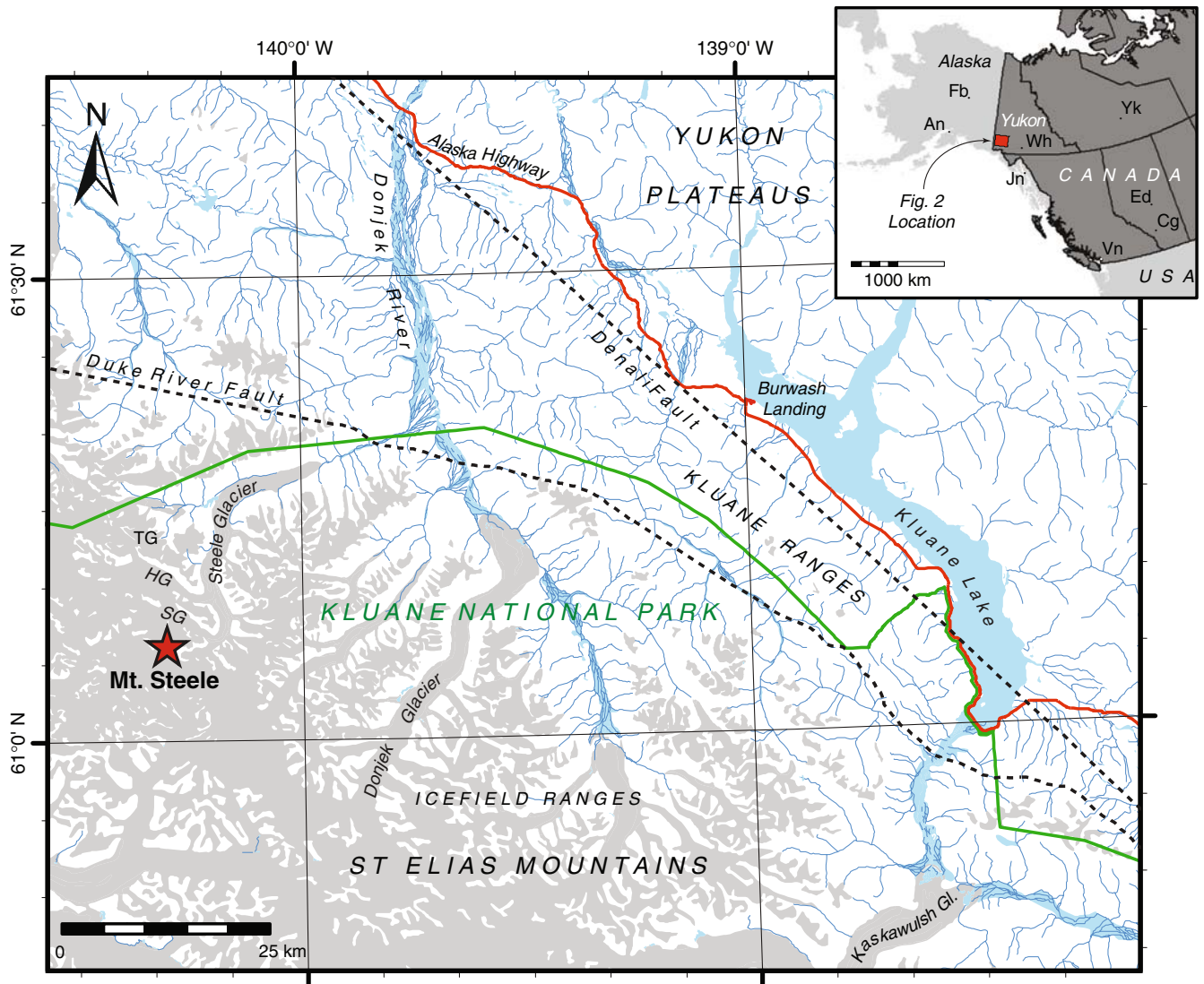


Fig. 2 Location of Mount Steele in southwestern Yukon, Canada. TG Trapridge Glacier, SG Steele Glacier, HG Hodgson Glacier. City abbreviations in inset map: Wh Whitehorse, Yk Yellowknife, Vn Vancouver, Cg Calgary, Ed Edmonton, An Anchorage, Fb Fairbanks, Jn Juneau

the main debris lobe was approximately 5 km from the source zone. The scientists photographed the deposit from the air on July 23 and 24, and additional small ice and snow avalanches were observed in the source zone during these visits. They estimated that 95% of the July 22 avalanche debris was highly fragmented ice and snow and 5% was rock debris; no large chunks of ice or rock were noted.

Seismographs in Alaska and northwestern Canada recorded the July 22 ice avalanche as a local magnitude (M_L) 2.1 seismic event. Based on the large difference between surface and body wave magnitudes, it was recognized as a mass movement rather than an earthquake (Ekström et al. 2007).

A larger mass movement (the “main event”) occurred at Mount Steele 2 days later, on July 24 at 1757 hours local time (Figs. 5c, 6c, d). It was not directly witnessed but was recorded on seismographs as a M_L 3.4 seismic event. The magnitude estimated from long-period surface-waves (M_s) is 5.2, and modeling of the waveforms suggests an estimated duration of 100 s (Ekström 2006; Ekström et al. 2007). Another, much smaller mass movement was detected by the Alaska

Earthquake Information Centre about 1.5 h later at the same location (N. Ruppert, personal communication, 2007). A prominent light-coloured (ice-rich) debris lobe located near the east margin of the deposit (Figs. 1 and 6c) is attributed to this secondary event and suggests that it was likely an ice avalanche.

Sixteen earthquakes were recorded within 300 km of Mount Steele between July 1 and 24, 2007, but none happened at or near the time of the July 22nd or July 24th mass movements. The largest and deepest of the earthquakes (M_L 4.1, depth 25 km) occurred on July 9; its epicentre was 152 km southeast of the mountain. The closest earthquake (M_L 2.3) occurred on July 2, 109 km east-southeast of Mount Steele. The other earthquakes ranged in size from M_L 2.0 to 3.7; their epicentres were 113 to 269 km south and southeast of Mount Steele, and their focal depths ranged from 1 to 15 km.

Analysis of Environment Canada air temperature records from Burwash Landing, located at 807 m elevation 76 km northeast of Mount Steele, indicates that daily average temperatures were up to 2.7°C above the 1971–2000 July monthly normal temperature (12.8°C) for 10 days prior to the main event. The average daily

Recent Landslides

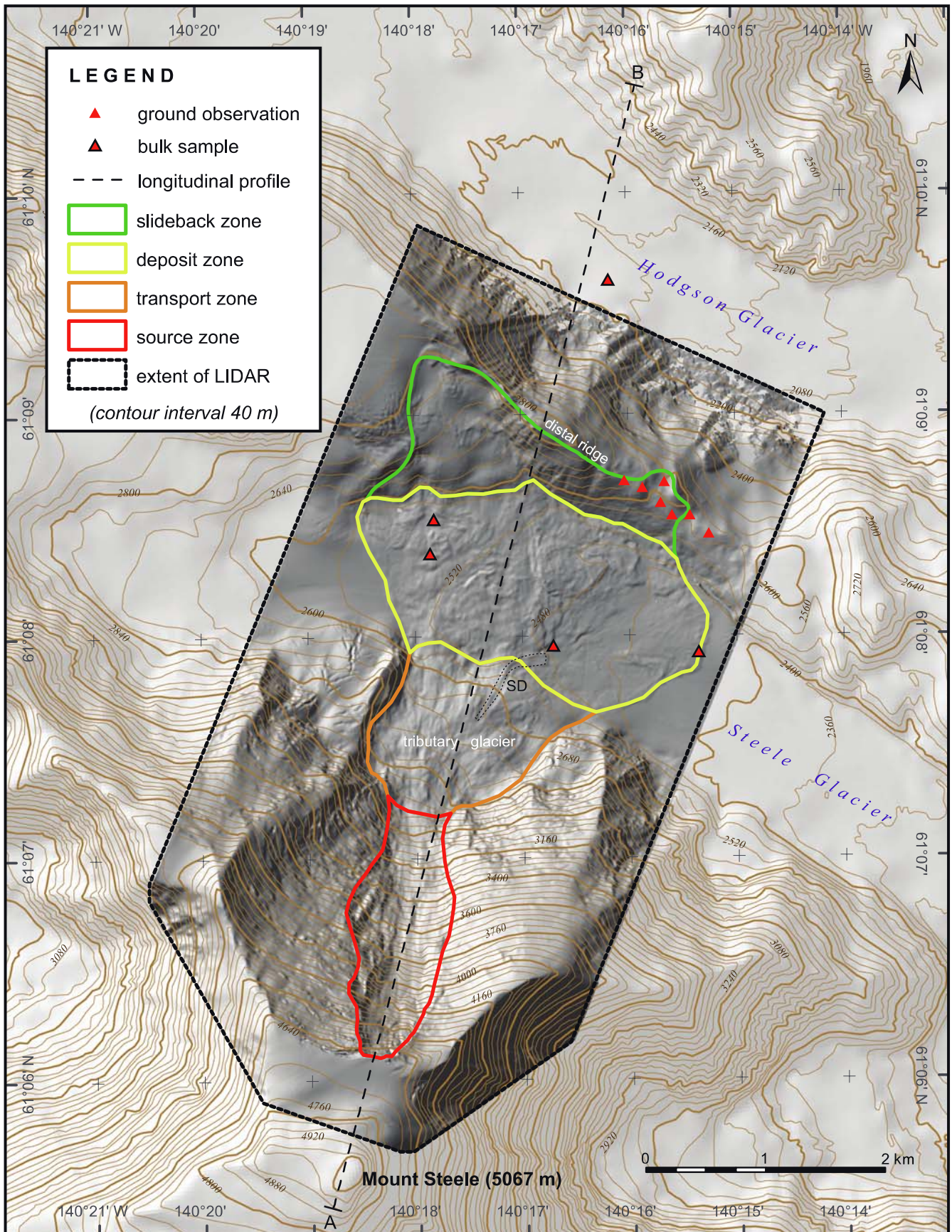


Fig. 3 Map of the July 24th rock and ice avalanche features. Hillshade image derived from the LiDAR survey described in the text. *SD* Secondary debris flow channel. The contours are from the pre-landslide topographic surface dating to 1951

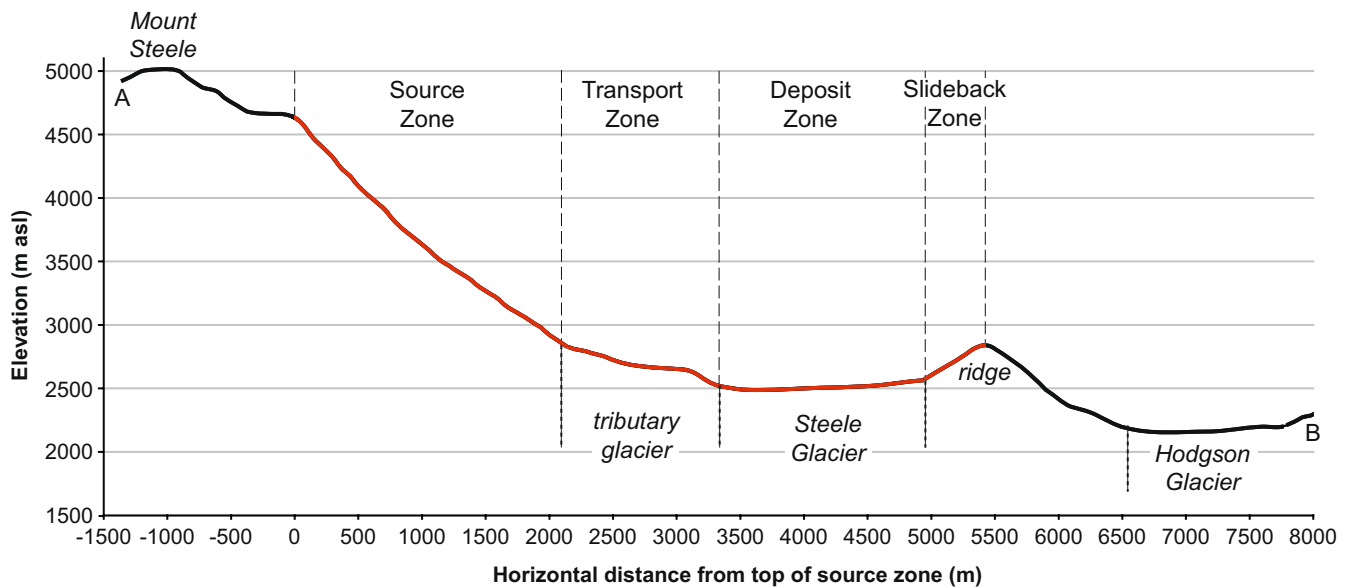


Fig. 4 Longitudinal profile along line A–B shown in Fig. 3. The travel path of the July 24th rock and ice avalanche is shown by the red line; this path is not equivalent to that used to determine maximum runout

temperature for the month of July was 0.6°C higher than normal; the average daily maximum temperature was 0.5°C lower than the 19.3°C normal; and the average daily minimum temperature was 1.5°C higher than the 6.3°C normal.

Following the main event, a number of field parties visited Mount Steele and documented key post-failure landslide characteristics. On July 25, geologists photographed the landslide debris and reported that “a lot of dust” was still in the air at 1400 hours (J. Spotila, personal communication, 2007). The Yukon Geological Survey conducted a fixed-wing reconnaissance survey on August 2 and revisited the site by helicopter on August 12 to obtain debris samples and additional photographs. The geologists observed small ice and snow avalanches initiating from different parts of the source zone during both visits.

A high-resolution, airborne LiDAR survey was conducted on August 12 by the Geological Survey of Canada in partnership with the Applied Geomatics Research Group (Centre of Geographic Sciences, Nova Scotia Community College). The survey was flown at altitudes between 4,000 and 6,100 m asl and at a flying speed of 260 km/h. Over seven million data points were collected along 11 east–west survey lines across the face of Mount Steele and adjacent Steele Glacier. A pulse frequency of 33 kHz, infrared laser wavelength of 1,064 nm and a scan angle of $\pm 24^\circ$ (48° field of view) were used. A hillshade digital elevation model derived from these data is shown as part of the background image in Fig. 3. Both the LiDAR survey data and 1:50,000-scale national topographic data (Natural Resources Canada) were used to characterize the topography of the landslide source area and deposit.

Characterization of the July 24th rock and ice avalanche

Failure and transport zones

The extreme upper portion of Mount Steele’s north face is covered by snow and ice and slopes 23–27° down from the summit (5,067 m asl) to a bench located at approximately 4,650 m asl (Fig. 1). The upper failure zone is delineated by a curved escarpment up to 540 m wide, which exposes approximately 70 m of ice above

bedrock along the edge of the bench. Below it, a steep (average slope 44°) gullied slope descends 1,750 m in elevation to a small tributary glacier that flows into Steele Glacier (Figs. 3 and 4). The rock and ice that failed during the main event extended from the headscarp down to the top of this tributary glacier.

Detailed examination of the failure zone was impossible due to the high altitude, extreme ruggedness of the terrain, ongoing landslide risk and snow cover. However, pebble- to boulder-sized fragments at the edge of the debris sheet and small rock fragments in bulk samples collected for analysis of particle size and water content indicate that the landslide occurred in light-coloured, hornblende-biotite-quartz diorite and tonalite and plagioclase-hornblende-biotite porphyry. The presence of slickensides, sericitic alteration of feldspars and red- to dark-brown oxidization of fracture surfaces suggests that the rocks originated from a fault zone.

Photographs of the failure zone indicate three main sets of discontinuities in the rock mass (Fig. 7). The most conspicuous discontinuity set (D1) consists of smooth planes striking parallel to and dipping at the same angle as the slope; some D1 planes may also daylight in the slope. The second discontinuity set (D2) dips in the same direction as D1, but at a steeper angle, and therefore does not daylight. The third discontinuity set (D3) is sub-vertical, strikes southwest to northeast, and probably controls the east lateral margin of the main scarp.

The transport zone of the landslide extends a horizontal distance of 1,350 m from the top of the tributary glacier at 2,900 m asl to the junction of the tributary glacier and Steele Glacier near 2,500 m asl (Figs. 1 and 3). Much of the original tributary glacier surface is visible in this zone; thus, only minor deposition occurred there. Where present, the debris was patchy and thin. Parts of the tributary glacier surface appear scoured in photographs taken shortly after the avalanche, and erosion was probably enhanced by pre-existing longitudinal crevasses. Analysis of the LiDAR data suggests that the most prominent scour is at least 16 m deep. The effects on landslide flow of surface roughness and the configuration of pre-existing longitudinal and transverse crevasses are uncertain.

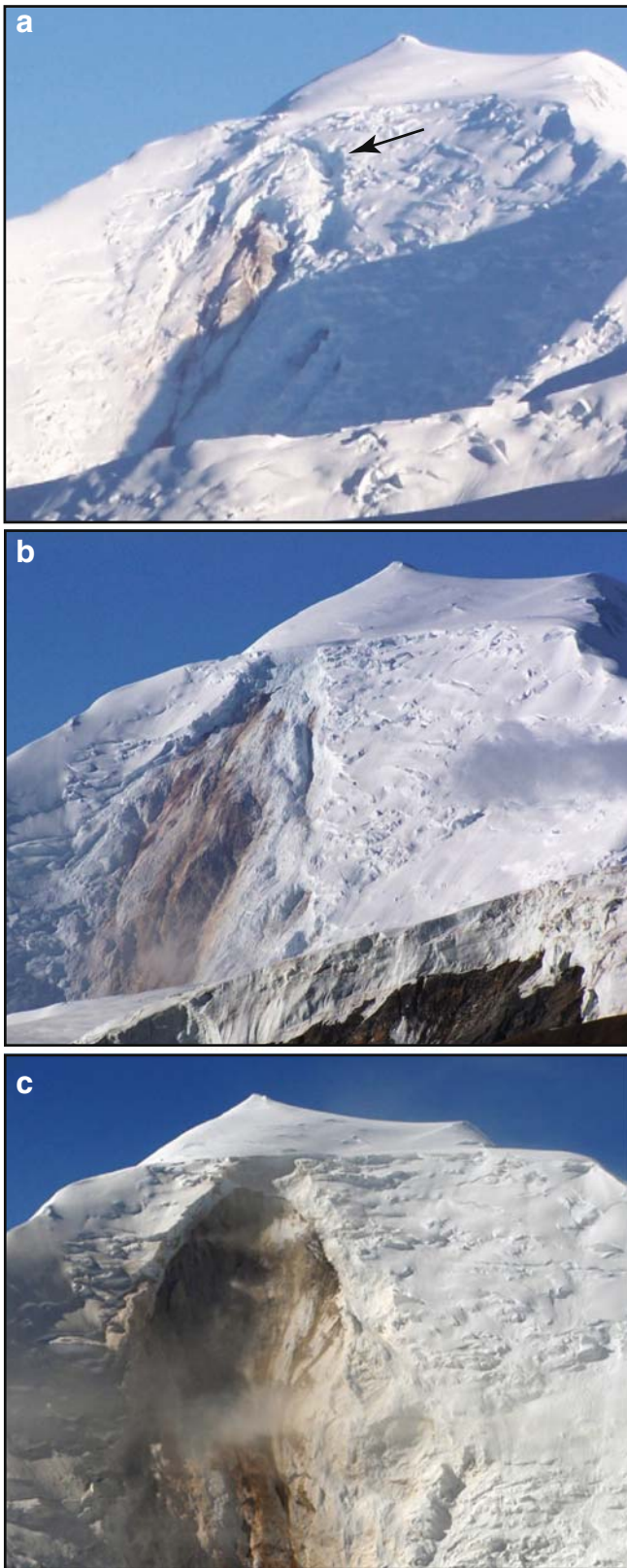


Fig. 5 Source zone of the ice and rock avalanches on the north face of Mount Steele. **a** Crevasse (arrow) outlining slab of ice that failed on July 22, 2007 (photo taken prior to July 22 by A. Schaeffer on July 15, 2007). **b** Bedrock exposed after the July 22 ice avalanche (photo by A. Schaeffer, July 23, 2007). **c** Source zone scar from July 24 main event; the scar is approximately 500 m wide (photo by P. von Gaza, August 2, 2007)

Fig. 6 Landslide deposits. **a** Fresh deposits of two or more small debris flows on tributary to Steele Glacier, prior to the main event; southern edge of Steele Glacier in the foreground (photo by L. Freese, July 21, 2007). **b** Deposit of July 22nd ice avalanche that extended across Steele Glacier; the deposit contains about 95% ice and 5% rock debris (photo by A. Schaeffer, July 24, 2007; view to west). **c** Debris of July 24th landslide; slideback zone is delineated by a dashed line. **d** Debris of July 24th rock and ice avalanche viewed from above the distal ridge that impeded runoff. Note the discontinuous thin debris on ridge crest and tributary glacier, the small ponds formed from ice melt (arrows) and secondary debris flow channel (SD; photo by P. Lipovsky, August 2, 2007)

Deposit zone

The July 24 avalanche deposited a sheet of ice and rock debris across the entire 1.5 km width of Steele Glacier. In the distal part of its path, the avalanche reached, but did not overtop, the crest of a 275-m-high ridge (Figs. 3 and 4). Some of the debris at the northwest edge of the deposit and much of the debris that climbed the ridge slid backwards on reverse slopes after reaching their limits of travel (Fig. 6c). We refer to this process as “slideback”. This is important to consider when attempting to estimate the thickness of debris on Steele Glacier, because it led to significant thickening of the debris at the base of the ridge.

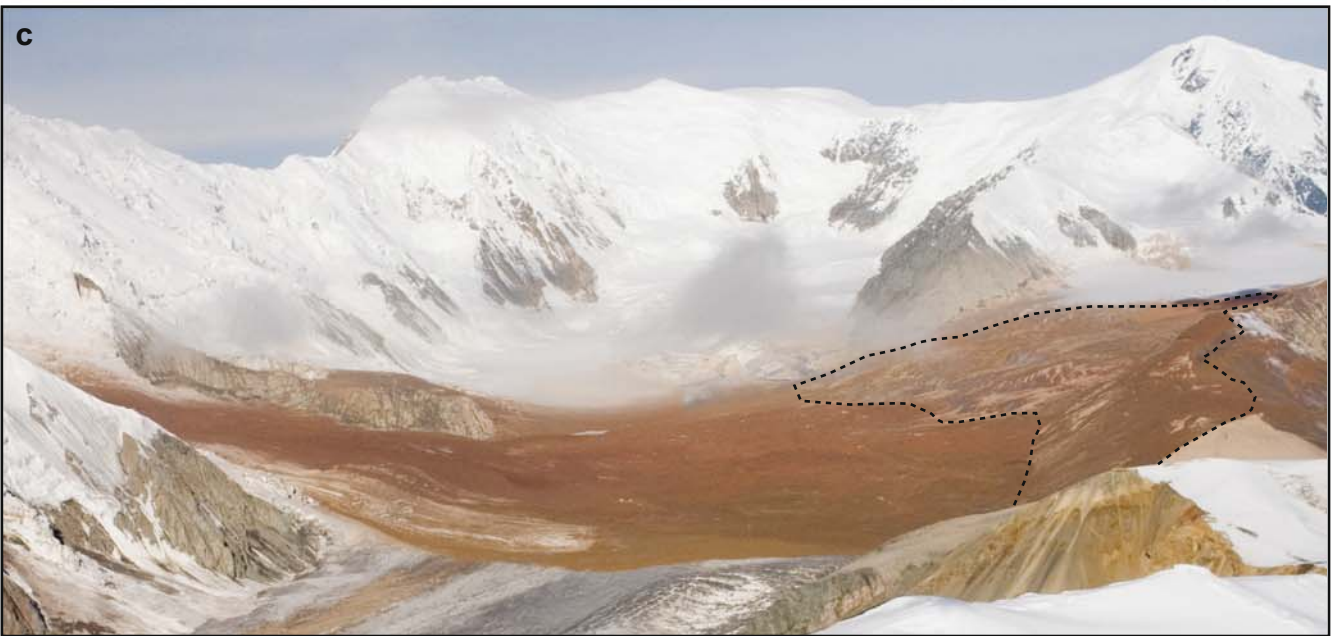
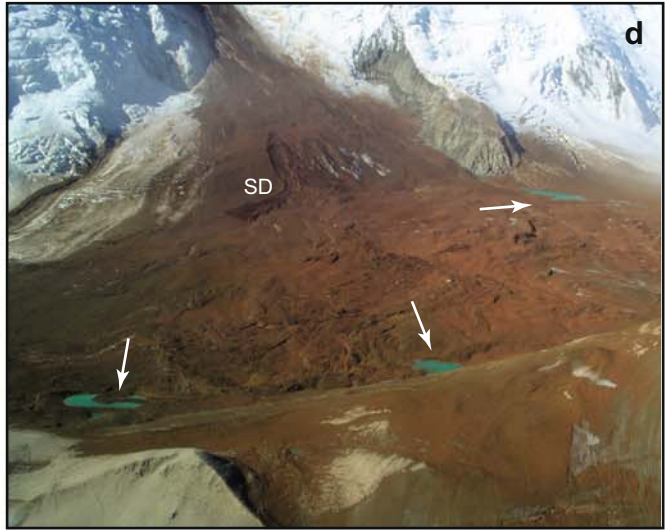
The debris sheet of the main event covered an area of 5.28 km², fanning out to a width of 3.1 km at the north margin of Steele Glacier (Fig. 3). This area includes the total area covered by debris before slideback. The area of slideback is about 1.62 km², thus the total area of significant debris cover is about 3.66 km².

The debris was thin on the south flank of the ridge that separates Steele and Hodgson glaciers and in places on Steele Glacier itself, notably where slideback occurred (Fig. 6c). Patchy, thin debris was also present over much of the tributary glacier, but this area is not included in the deposit zone shown in Fig. 3 since debris transport dominated in this part of the path. In addition, a coating of airborne silt and sand up to 20 cm thick accumulated above snow and ice on both sides of the ridge crest, and this material was not considered part of the main debris sheet.

The surface of the debris sheet was hummocky, and the local relief of the hummocks, estimated during aerial surveys, was up to 10 m. No surface water was visible within the debris sheet in photographs taken on July 25, but numerous small ponds had developed on and adjacent to the debris sheet by August 2 (Fig. 6d). Photographs of the Steele Glacier surface taken before the main event indicate very little supraglacial surface water that could have been dammed by the debris and contributed to the ponding, suggesting that the debris contained a significant volume of ice that quickly melted during transport and/or after deposition. Photographs taken less than a day after the main event indicate a prominent secondary debris flow channel near the southern margin of the debris sheet (Fig. 6d), further suggesting that the debris was highly saturated when it was deposited.

The debris is much finer than typical rock avalanche deposits (Evans and Clague 1988, 1999; Jibson et al. 2006). Only scattered boulders were observed during the helicopter surveys, and none was larger than 3 m in size. The high degree of fragmentation suggests that the source rock may have been intensely fractured before it failed.

Bulk samples (3.5–4 kg) of surface debris were collected at four locations on August 12 (Fig. 3). The solid portion of the samples consists of 58–64% coarse-grained material (>2 mm), the majority



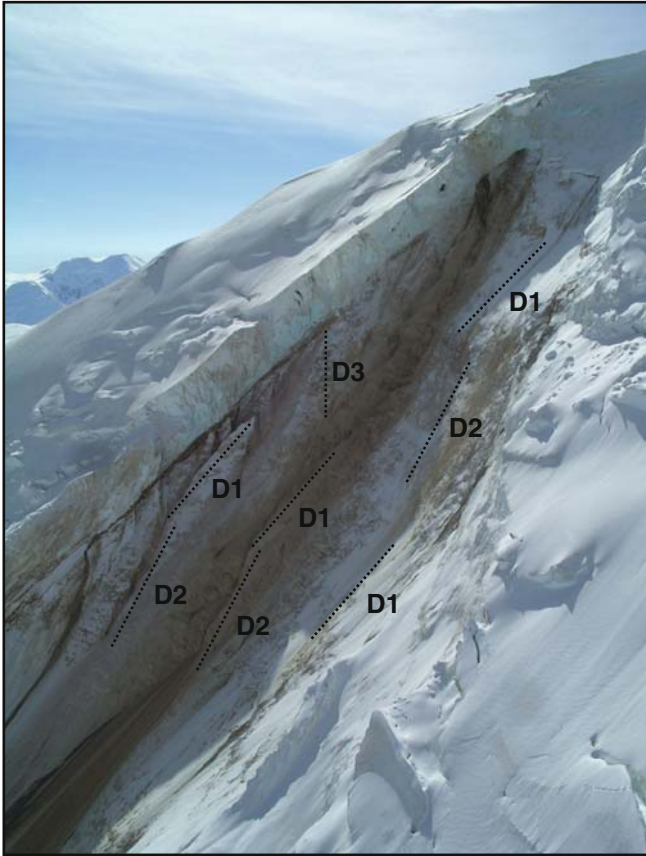


Fig. 7 Discontinuities (D1, D2 and D3) in the rock mass of the July 24th rock and ice avalanche source zone (photo by P. Lipovsky, August 12, 2007)

of which is pebble-size. The remaining fine-grained material consists of 72–75% sand, 19–21% silt and 7–9% clay. Water constituted 7–35% of the mass of the samples and is assumed to have originally been snow and ice. Based on these data, the debris sheet must have contained significant volumes of snow and ice at the time of the rock avalanche nearly 3 weeks earlier. Several large ice blocks, up to 2 m across, were also observed near the crest of the ridge separating Steele and Hodgson glaciers on August 12.

We did not attempt to characterize or map the debris on the ground during the 2007 field season because of the continuing high hazard at the site. The area of the deposit is accurately known from the LiDAR survey, but some uncertainty remains concerning the maximum and mean thicknesses of the debris and therefore its volume. This uncertainty is primarily due to the fact that the surface elevation and morphology of the Steele Glacier immediately prior to the main event is not adequately known. The only topographic map available for the Mount Steele area was produced from 1951 aerial photography. Subsequent changes in the surface elevation of Steele Glacier are difficult to estimate because of the strong influence of sporadic surging events. Based on visual inspection during the helicopter survey on August 12, the debris appeared to range in thickness from 4 to 15 m, suggesting an average thickness of about 7.5 m. LiDAR mapping indicates a greater average thickness, on the order of 22 m. These average thickness values imply volumes of 27.5 and 80.5 Mm³, respectively, for the main event, and include a significant volume of ice. These values are minimum and maximum estimates of the main event

deposit volume. Future field work will refine these estimates of debris thickness and volume.

Dynamic reconstruction

The mean velocity of the main event was estimated from seismograms recorded at US Geological Survey seismic stations in Alaska on July 24th. The seismograms indicate that the event lasted for approximately 100 s, a duration which may include slideback motion after the maximum runout distance had been reached. The path distance to the distal edge of the slideback zone varies between 6.5 and 3.5 km depending on whether it is measured from the top of the landslide source zone or the base of the source zone, respectively. The average velocity over the maximum and minimum path distances is therefore between 65 and 35 m/s, respectively. The debris run-up (h) to the summit of the distal ridge was about 275 m (Fig. 4). For this run-up geometry, the energy head formula ($v = [2gh]^{-2}$) gives a minimum velocity (necessary to overtop the ridge) of 73 m/s at a horizontal distance of 5,000 m.

A first-order, 2-D dynamic analysis of the main event along the path shown in Fig. 4 was carried out using the simulation software DAN (Hungr 1995; Hungr and McDougall 2008). In the DAN model, debris width (taken from Fig. 3) is input along the path length of the rock avalanche. The simulation was carried out for material which originated in the source zone as defined in Fig. 4, using an initial failure volume of 51 Mm³, in the mid-range of our volume estimates noted above. No entrainment was specified since there is no evidence of significant debris entrainment along the path of the main event. Defining the origin of the landslide as the base of the source zone, the run time and the run-out distance of the debris front were simulated very well (Fig. 8) using a Voellmy basal resistance model (Hungr 1995) with values of 0.052 and 1,525 m/s² for the friction (μ) and turbulence coefficients (ξ), respectively. These parameter values are comparable to those used to successfully simulate the 1964 Sherman Glacier rock avalanche ($\mu = 0.03$ and $\xi = 1,000$ m/s²; Hungr and Evans 1996). The run-up to the top of the ridge is simulated almost precisely, without overtopping it, and the slideback is also predicted (Fig. 8). The simulated velocity at a horizontal distance of 5,000 m is 42 m/s, which is significantly lower than the 73 m/s estimated from the energy head formula.

The travel angle [$\text{fahrböschung} = \arctan(H/L)$] of the Mount Steele main event is 18°, where $H = 1,860$ m and $L = 5,760$ m. In this case, both H and L were measured to the most distal edge of the slideback zone (i.e. to the maximum limit of debris travel). It should be noted, however, that the maximum descent from the headscarp to the surface of Steele Glacier is 2,160 m. The H/L ratio for the Mount Steele event is the largest for 20 rock avalanches documented with volumes greater than 1 Mm³ and which occurred onto glaciers in northwest North America (Alaska, Yukon, British Columbia) between 1956 and 2007 (Fig. 9; Evans and Clague 1988, 1999; Jibson et al. 2006; Molnia et al. 2006). The anomalously low mobility of the main event resulted from impact of the debris with the distal ridge and the spreading of debris on the surface of Steele Glacier. We point out, however, that the debris exhibited reverse mobility by sliding back onto the surface of Steele Glacier. This debris probably collided with material still moving down the path in the initial movement direction. We suggest this process also contributed to the chaotic surface topography of the debris in the deposit zone.

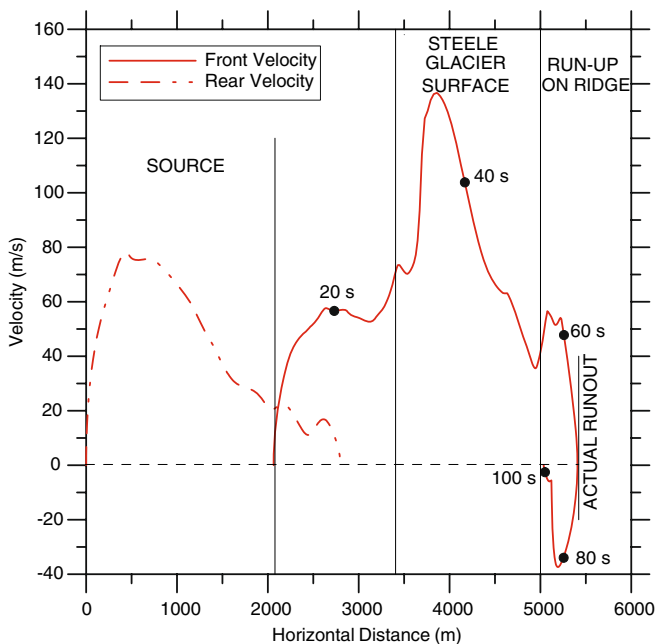


Fig. 8 Simulated velocity profile of the main event rock and ice avalanche on July 24th, 2007. The velocity of the front and rear of the debris sheet are shown. Note the rapid acceleration of the debris when the front of the sheet encounters the surface of Steele Glacier, followed by rapid deceleration as the debris thins and spreads out on the glacier surface. The black dots represent position and velocity of the debris front at 20 s intervals during movement. Maximum runout was achieved at 69 s, suggesting a simulated mean velocity of 78 m/s. By 100 s, the slideback of debris had reached the base of the ridge. Simulation was carried out using the Voellmy model in DAN (Hungry 1995) with values of 0.052 and 1,525 m/s^2 for the friction and turbulence coefficients, respectively

Global comparisons of occurrence and behaviour

Rock avalanches onto glaciers are common in high glacierized mountain ranges of the world (Evans and Clague 1988; Petrakov et al. 2008) and have been well-documented in the European Alps (Eisbacher and Clague 1984; Porter and Orombelli 1980), the Southern Alps of New Zealand (McSaveney 2002), the Himalayas (Hewitt, 2008), the Cordillera of northwest North America (Post 1967; Evans and Clague 1999; Jibson et al. 2006; Molnia et al. 2006) and the Andes (Hauser 2002). They form part of a spectrum of complex mass movement processes involving glacial ice (Petrakov et al. 2008) that are significant hazards in some mountain terrain.

Rock avalanches and related mass movements that are contained within the limits of a glacier normally pose little risk to people and infrastructure. In contrast, mass movements that evolve, either instantaneously or after some delay, from rock and ice avalanches onto glacier surfaces and travel beyond glacier limits have caused disasters in populated mountain ranges. One of the most deadly landslides in recent times developed from an earthquake-triggered rock and ice avalanche that fell from the north peak of Nevado Huascaran onto a glacier surface in the Cordillera Blanca, Peru in 1970 (Pflaker and Ericksen 1978; Evans et al. 2007). The landslide obliterated the town of Yungay, claiming thousands of lives (Cluff 1971; Keefer and Larsen 2007).

Glacier-related mass movements commonly involve flows of highly fragmented, ice-laden debris that travel long distances reaching very high maximum velocities, that in some cases exceed 100 m/s (Evans et al. 1989; Petrakov et al. 2008). As in the Mount

Steele case, melt of ice and snow at the base of the moving mass and that which was incorporated during movement contributes to the high mobility and velocities of these landslides.

The runout of rock avalanches on glaciers is commonly enhanced compared to that of non-glacial rock avalanches of the same volume (Evans and Clague 1988, 1999). However, the runout of the main event at Mount Steele was significantly less than other rock avalanches of similar volume that have occurred on glaciers (Fig. 9; Evans and Clague 1988, 1999; Jibson et al. 2006; Molnia et al. 2006). In the Mount Steele case, runout was impeded when the landslide encountered a significant topographic barrier—the 275-m-high ridge separating Steele and Hodgson glaciers (Figs. 2 and 3). In addition, the Mount Steele landslide, although initially guided by ravines on the north flank of the mountain, subsequently spread over the nearly flat surface of Steele Glacier, dissipating much of its energy. The combination of a topographic barrier and rapid unconfined spreading of the debris on the glacier surface explains the relatively short travel distance of the landslide in relation to its volume.

Conclusions

The Mount Steele rock and ice avalanche, which occurred on July 24, 2007, ranks among the largest documented landslides in the mountains of western Canada. It was part of a sequence of slope failures that occurred on the north slope of Mount Steele over a period of several days in July 2007. Further research is needed to determine whether these events were causally related. None of the failures were triggered by earthquakes. Weather records from the closest community of Burwash Landing suggest that air temperatures in July 2007 were not anomalous in the region. The failures occurred on a slope that has been the source of previous slope instability. The fine texture and the red-brown colour of the debris suggest that the igneous rocks in the failure zone are highly sheared and have low rock mass strength, perhaps because they lie within a fault zone.

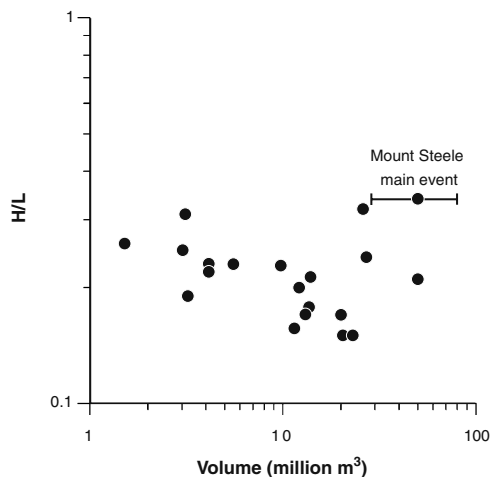


Fig. 9 Comparison of Mount Steele main event mobility with 20 rock avalanches (volume $>1 \text{ Mm}^3$) onto glaciers documented in northwest North America (Alaska, Yukon and British Columbia) between 1956 and 2007. H/L is defined in the text, and the volume of the main event is plotted as the mid-point between the minimum and maximum volume estimates described in the text. Data are from Evans and Clague (1988 and 1999), Jibson et al. (2006) and Molnia et al. (2006)

Despite the remote location, the July events were exceptionally well-documented by eyewitnesses and seismographs. Analysis of seismic records indicates a maximum and minimum mean velocity of 65 and 35 m/s, respectively, for the main event. During this event, ice and rock debris descended a maximum of 2,160 vertical metres and traveled a maximum horizontal distance of 5.76 km. Runout was impeded by a 275-m-high ridge on the north side of Steele Glacier; the leading edge of debris just reached the top of the ridge before it slid back onto Steele Glacier. The debris contained much snow and ice derived from the slopes of Mount Steele. The melting of the entrained snow and ice contributed to the fluidity of the debris, its mobility and its high velocity. The Mount Steele landslide is one of a large number of landslides onto glaciers over the past century in northwestern North America, indicating that rock slopes adjacent to glaciers are particularly prone to catastrophic failure. Work is ongoing in order to evaluate the causes of the Mount Steele landslide sequence and to characterize the geometry and behaviour of the July 24th event with more precision.

Acknowledgements

We gratefully acknowledge contributions to this study made by Steve Israel (Yukon Geological Survey); Peter von Gaza (Pixel Mapper Geoscience); Doug Makkonen (Trans North Helicopters); Lance Goodwin, Andy Williams and Donjek Upton (Icefield Ranges Expeditions); Dr. John Barlow and the Canadian Consortium for LiDAR Environmental Applications Research (C-CLEAR) field crew; Lloyd Freese (Kluane National Park); Christian Zdanowicz (Geological Survey of Canada); Dr. Natalia Ruppert (Alaska Earthquake Information Center, University of Alaska Fairbanks); and Dr. Gerald Holdsworth (Arctic Institute of North America, University of Calgary). Stephen A. Wolfe provided a Geological Survey of Canada internal review. We also acknowledge the helpful reviews of Dr. Patrick Wassmer and an anonymous reviewer. We acknowledge Natural Resources Canada Earth Sciences Sector contribution number 20070457.

References

Bruhn RL, Pavlis T, Plafker G, Serpa L (2004) Deformation during terrane accretion in the Saint Elias orogen, Alaska. *Geol Soc Am Bull* 116(7–8):771–787

Clague JJ (1979) The Denali Fault system in southwest Yukon Territory—a geologic hazard? In: *Current Research Part A, Geological Survey of Canada, Paper 79-1A*, pp 169–178

Cluff LS (1971) Peru earthquake of May 31, 1970; engineering geology observations. *Bull Seismol Soc Am* 61:511–533

Dodds CJ, Campbell RB (1992) Geology of Mount St. Elias map area (115B and F[E1/2]), Yukon Territory. Geological Survey of Canada Open File 2189

Eisbacher GH, Clague JJ (1984) Destructive mass movements in high mountains. Geological Survey of Canada Paper 84-16, 228 pp

Ekström G (2006) Global detection and location of seismic sources using surface waves. *Bull Seismol Soc Am* 96(4A):1201–1212

Ekström G, Hansen RA, Pavlis GL, Lipovsky PL (2007) Seismological detection and analysis of recent landslides in Alaska and the Yukon. In: *Eos Trans. AGU, 88(52)*, Fall Meet. Suppl., Abstract S52B-05

Evans SG, Clague JJ (1988) Catastrophic rock avalanches in glacial environments. In: *Bonnard C (ed) Proceedings of the 5th International Symposium on Landslides, Lausanne*, 2:1153–1158

Evans SG, Clague JJ (1999) Rock avalanches on glaciers in the Coast and St. Elias Mountains, British Columbia. In: *Proceedings of the 13th Annual Vancouver Geotechnical Society Symposium, Vancouver*, pp 115–123

Evans SG, Clague JJ, Woodsworth GJ, Hungr O (1989) The Pandemonium Creek rock avalanche, British Columbia. *Can Geotech J* 26(3):427–446

Evans SG, Fidel SL, Zegarra LJ (2007) Los Movimientos en Masa de 1962 y 1970 en el Nevado de Huascarán, Valle del río Santa, Cordillera Blanca, Perú. Anexo B4. In: *Movimientos en Masa en la Región Andina: Una guía para la evaluación de amenazas. Proyecto Multinacional Andino: Geociencias para las Comunidades Andinas, Publicación Geológica Multinacional, No. 4*, pp 386–404

Everard KA, Savigny KW (1994) Neotectonic effects of landslide distributions, Yukon, Canada. In: *Oliveira R, Rodrigues LF, Coelho AG, Cunha AP (eds) Proceedings, 7th International Congress. International Association of Engineering Geology, Lisbon*, pp 1811–1820

Grady SP, Makepeace AJ (2003) Yukon digital geology, version 2.0. *Geol Surv Canada Open File 1749 and Yukon Geological Survey Open File 2003-9(D)*, 2 CD-ROMS

Haeussler PJ, Schwartz DP, Dawson TE, Stenner HD, Lienkaemper JJ, Sherrid B, Cinit FR, Montone P, Craw PA, Crone AJ, Personius SF (2004) Surface rupture and slip distribution of the Denali and Totshunda faults in the 3 November 2002 M7.9 earthquake, Alaska. *Bull Seismol Soc Am* 94(6B):S23–S52

Hauser A (2002) Rock avalanche and resulting debris flow in Estero Parraguire and Rio Colorado, Region Metropolitana, Chile. In: *Evans SG, DeGraff JV (eds) Catastrophic landslides: effects, occurrence and mechanisms. Geological Society of America Reviews in Engineering Geology* 15:135–148

Hewitt K (2008) Rock avalanches that travel onto glaciers and related developments, Karakoram Himalaya, Inner Asia. *Geomorphology* (in press)

Horner RB (1983) Seismicity in the St. Elias region of northwestern Canada and southeastern Alaska. *Bull Seismol Soc Am* 73:1117–1137

Hungr O (1995) A model for the runout analysis of rapid flow slides, debris flows and avalanches. *Can Geotech J* 32:610–623

Hungr O, Evans SG (1996) Rock avalanche runout prediction using a dynamic model. In: *Proceedings of the 7th International Symposium on Landslides, Trondheim*, 17–21 June 1996, pp 233–238

Hungr O, McDougall S (2008) Two numerical models for landslide dynamic analysis. *Computers and Geosciences*, doi:10.1016/j.cageo.2007.12.003

Jibson RW, Harp EL, Schulz W, Keefer DK (2006) Large rock avalanches triggered by the M 7.9 Denali Fault, Alaska, earthquake of 3 November 2002. *Eng Geol* 83:144–160

Keefer DK, Larsen MC (2007) Assessing landslide hazards. *Science* 316:1136–1138

Lowe GW (1998) A new estimate of the amount of displacement on the Denali Fault system based on the occurrence of carbonate megaboulders in the Dezadeash Formation (Jura-Cretaceous), Yukon, and the Nutzotin Mountains sequence (Jura-Cretaceous), Alaska. *Bull Can Pet Geol* 46(3):379–386

McSaveney MJ (2002) Recent rockfalls and rock avalanches in Mount Cook National Park, New Zealand. In: *Evans SG, DeGraff JV (eds) Catastrophic landslides: effects, occurrence and mechanisms. Geological Society of America, Reviews in Engineering Geology*, 15:35–70

Molnia BF, Agnelli KM, Bratton DA, Keeler RH, Noyles C (2006) Meltwater induced glacier landslides—Waxell Ridge, AK. *Eos* 87(52), Fall Meeting Supplement, Abstract C31A-1247

Pavlis TL, Picornell C, Serpa L, Bruhn RL, Plafker G (2004) Tectonic processes during oblique collision: insights from the St. Elias orogen, northern North American Cordillera. *Tectonics* 23(3):1–14

Petrakov D, Chernomoretz SS, Evans SG, Tutubalina OV (2008) Catastrophic multi-phase glacial movement: a special type of glacier hazard. *Adv Geosci* 14:211–218

Pflaker G, Erickson GE (1978) Nevados Huascarán avalanche, Peru. In: *Voight B (ed) Rockslides and avalanches, Volume 1: natural phenomena. Elsevier, New York*, pp 277–314

Porter SC, Orombelli G (1980) Catastrophic rockfall of September 12, 1717 on the Italian flank of the Mont Blanc massif. *Z Geomorphol* 24:200–218

Post A (1967) The Alaska earthquake March 27, 1964: effects on hydrologic regimen. U. S. Geological Survey Professional Paper 544-D

Smith CAS, Meikle JC, Roots CF (eds) (2004) *Ecoregions of the Yukon Territory: biophysical properties of Yukon landscapes. Agriculture and Agri-Food Canada, PARC Technical Bulletin No. 04-01, Summerland, BC*, 313 pp

Spotila JA, Buscher JT, Meigs AJ, Reiners PW (2004) Long-term glacial erosion of active mountain belts: examples of the Chugach-St Elias Range, Alaska. *Geology* 32(6):501–504

Stanley AD (1969) Observations of the surge of Steele Glacier, Yukon Territory, Canada. *Can J Earth Sci* 6(4):819–830

Stanley AD (1972) Observations of the surge of Steele Glacier. In: *Bushnell VC, Ragle RH (eds) Icefield Ranges Research Project scientific results, volume 3. American Geographical Society and Arctic Institute of North America*, pp 61–69

Wheeler JO, Brookfield AJ, Gabrielse H, Monger JW, Tipper HW, Woodsworth GJ (compilers) (1991) *Terrane map of the Canadian Cordillera, Geological Survey of Canada Map 1713A, scale 1:2 000 000*

Wood WA (1972) Steele Glacier, 1935–1968. In: Bushnell VC, Ragle RH (eds) Icefield Ranges Research Project scientific results, volume 3. American Geographical Society and Arctic Institute of North America, pp 1–8

P. S. Lipovsky (✉)

Yukon Geological Survey, Government of Yukon,
2099 2nd Avenue,
Whitehorse, Yukon Y1A 2C6, Canada
e-mail: Panya.Lipovsky@gov.yk.ca

S. G. Evans · K. B. Delaney · N. J. Roberts

Landslide Research Programme, Department of Earth and Environmental Sciences,
University of Waterloo,
200 University Avenue West,
Waterloo, Ontario N2L 3G1, Canada

J. J. Clague

Centre for Natural Hazard Research, Department of Earth Sciences,
Simon Fraser University,
8888 University Drive,
Burnaby, British Columbia V5A 1S6, Canada

C. Hopkinson

Applied Geomatics Research Group, Centre of Geographic Sciences,
Nova Scotia Community College,
50 Elliott Rd, RR1,
Lawrencetown, Nova Scotia B0S 1M0, Canada

R. Couture · P. Bobrowsky

Geological Survey of Canada (Landslides and Geotechnics),
Natural Resources Canada,
601 Booth Street,
Ottawa, Ontario K1A 0E8, Canada

G. Ekström

Lamont-Doherty Earth Observatory, Columbia University,
61 Route 9W,
Palisades, NY 10964, USA

M. N. Demuth

Geological Survey of Canada (Glaciology), Natural Resources Canada,
601 Booth Street,
Ottawa, Ontario K1A 0E8, Canada

G. Clarke · A. Schaeffer

Department of Earth and Ocean Sciences,
University of British Columbia,
6339 Stores Road,
Vancouver, British Columbia V6T 1Z4, Canada